

Fragility of local moments against hybridization with singular baths

Max Fischer,¹ Arianna Poli,² Lorenzo Crippa,^{1,3} Sergio Ciuchi,²
Matthias Vojtá,⁴ Alessandro Toschi,⁵ and Giorgio Sangiovanni¹

¹*Institut für Theoretische Physik und Astrophysik and Würzburg-Dresden Cluster of Excellence ct.qmat, Universität Würzburg, 97074 Würzburg, Germany*

²*Dipartimento di Scienze Fisiche e Chimiche, Università dell'Aquila, Coppito-L'Aquila, Italy*

³*I. Institute of Theoretical Physics, Universität Hamburg, Notkestraße 9-11, 22607 Hamburg, Germany*

⁴*Institut für Theoretische Physik und Würzburg-Dresden Cluster of Excellence ct.qmat, Technische Universität Dresden, 01062 Dresden, Germany*

⁵*Institute of Solid State Physics, TU Wien, 1040 Vienna, Austria*

(Dated: March 19, 2025)

The Kondo screening of a localized magnetic moment crucially depends on the spectral properties of the electronic bath to which it is coupled. While textbook examples typically assume a hybridization being constant in energy, realistic systems as well as dynamical mean-field theories of correlated lattice models force us to consider also sharp features in the hybridization function near the Fermi energy ε_F . A case currently under the spotlight is twisted bilayer graphene where strongly correlated bands and their coupling to more itinerant ones make the effective hybridization function diverge at Dirac-point energies. To clarify the fundamental screening mechanisms at play in these less conventional impurity models, we consider a minimal Anderson impurity model featuring a bath density of states consisting of a regular part plus a tunable δ -function. Our analysis unveils an unexpectedly big impact on the physics of the Kondo screening already for a parametrically small weight of the δ -function contribution.

The Kondo effect is a low-temperature many-body phenomenon that arises in the presence of time-reversal symmetry when a quantum “impurity” spin is in contact with a metallic background of free electrons [1, 2]. An antiferromagnetic exchange coupling between the itinerant electrons and the impurity degrees of freedom leads to the formation of singlet states, screening the localized spin below the Kondo temperature T_K . This many-body state influences transport not only in metals with local moments, but also in synthetic nanostructures where the Coulomb blockade in quantum dots enables the control of magnetic moments and their screening [3–6].

Microscopically, a general approach to Kondo physics is in terms of the Anderson impurity Hamiltonian [7]. This describes both the itinerant bath and the localized degrees of freedom as electrons and couples these two fermionic species via $\Delta(\omega)$, i.e. a complex “hybridization” function of frequency. In order to facilitate analytical studies of the Anderson impurity model (AIM), assumptions frequently made are: *i*) the infinite-bandwidth limit for the bath, i.e., $\Lambda \rightarrow \infty$ in Fig. 1, *ii*) strongly suppressed charge fluctuations on the impurity, such that the impurity behaves as a true spin, and *iii*) the single-orbital nature of the impurity, implying a spin $S = 1/2$. In numerical studies, e.g. via quantum Monte Carlo methods, these assumptions are often relaxed [8–12].

In contrast, the functional form of $\Delta(\omega)$ is traditionally less versatile, especially within model studies of the Kondo effect. The hybridization function close to the Fermi level ε_F is either assumed to be smooth and slowly varying (a perfect constant would correspond to $\alpha=0$ in Fig. 1), or is taken of pseudogap form, vanishing as a power law in $(\omega - \varepsilon_F)$ [14, 15]. Yet, the recent surge

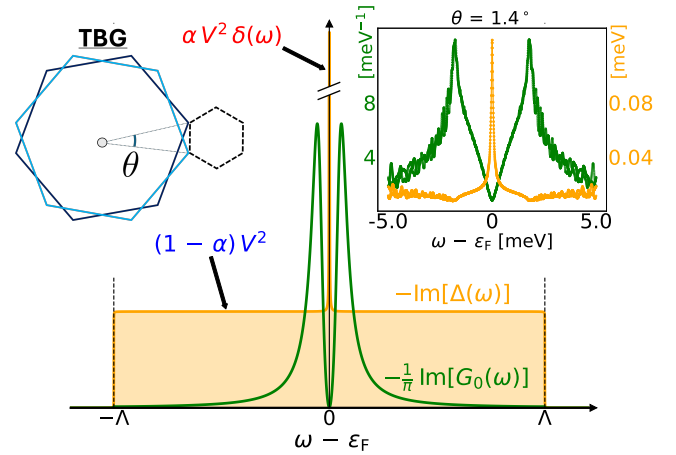


FIG. 1. (main panel) Toy-model hybridization function $\text{Im}\Delta(\omega)$ (orange) of an AIM, Eq. (1), and corresponding non-interacting spectral function at the impurity site $-\text{Im}G_0(\omega)/\pi$ (green). The latter vanishes quadratically close to the Fermi energy ε_F for every finite α , the parameter tuning the weight of the δ -like feature in the hybridization with respect to the constant background. Varying $\alpha \in [0 : 1]$ interpolates between the conventional “box”-like hybridization function ($\alpha=0$) and a single bath level ($\alpha=1$). Left inset: schematic of the Moiré Brillouin zone of twisted bilayer graphene. Right inset: hybridization function and non-interacting spectral function for the THF model of TBG at $\theta = 1.4^\circ$ [13].

of interest in the Moiré physics of twisted bilayer van der Waals materials calls for an urgent reconsideration of the impact of singularities in $\text{Im}\Delta(\omega)$. Indeed, twisted bilayer graphene (TBG) can be described within a so-called topological heavy-fermion (THF) periodic Ander-

son model [16–20] in which the more localized bands form Dirac cones of extremely reduced bandwidth. Then the effective hybridization function, obtained within a dynamical mean-field theory (DMFT) approximation [21], develops a singularity, located at ε_F for integer filling, superimposed to a more regular background, as shown in the right inset of Fig. 1.

Singular hybridization model.— In this Letter, we focus on single-impurity physics and model the peculiar form of $\text{Im}\Delta(\omega)$ by means of a simplified single-orbital hybridization (orange line in the main panel of Fig. 1):

$$-\frac{1}{\pi} \text{Im}\Delta(\omega) = (1 - \alpha) V^2 \text{rect}\left(\frac{\omega}{2\Lambda}\right) + \alpha V^2 \delta(\omega). \quad (1)$$

The parameter α controls the relative weight between the “box”-like regular part with energy cutoff Λ and the δ function at $\varepsilon_F = 0$, and V^2 is the overall strength of the hybridization between the local impurity and the bath. The corresponding non-interacting impurity Green’s function $G_0(\omega)$ of the AIM is obtained via

$$G_0^{-1}(\omega) = \omega + i0^+ + \mu - \Delta(\omega), \quad (2)$$

implicitly assuming a single-orbital local impurity. From Eq. (2) one sees immediately the connection between the singularity in $\Delta(\omega)$ and the vanishing of $\text{Im}G_0(\omega)$ as captured by our toy model [22]. We recall that, within DMFT, the impurity Green’s function G_0 is identified with the local Green’s function of the underlying lattice system. In the following, we will use the results obtained from an AIM with hybridization as in Eq. (1) to draw general conclusions concerning the consequences of the bath singularity for Kondo screening: As shown below, the behavior is surprisingly sensitive to the parameter α , i.e., even a small weight of the singular component dramatically alters the conventional screening scenario.

It is worth pointing out that zero spectral weight for G_0 at ε_F and an accompanying singularity in the hybridization Δ are not uncommon in DMFT settings. For example, they occur in the Kondo-insulating phase of the periodic Anderson model [23] as well as in three-dimensional Dirac semimetals [24, 25], both cases resulting in a $\delta(\omega)$ peak in $\text{Im}\Delta(\omega)$. Spikes in $\text{Im}\Delta(\omega)$ close to the Fermi level appear also in molecular systems, such as transition-metal phthalocyanines adsorbed on Ag(001) surfaces. These exhibit in the case of Mn, a fairly sharp peak in the hybridization for the xz/yz orbitals, superimposed to the rather constant z^2 contribution (see e.g. [26]). Nevertheless, the effects of a singular $\text{Im}\Delta(\omega)$ on the physics of the AIM have not been analyzed in detail hitherto. We note that Kondo-type models with a bath density of states diverging at the Fermi level have been investigated before in Refs. 27 and 28. However, the focus there was on pure power-law divergencies which are not relevant for the situations described above.

Before presenting the solution of the AIM (1) which

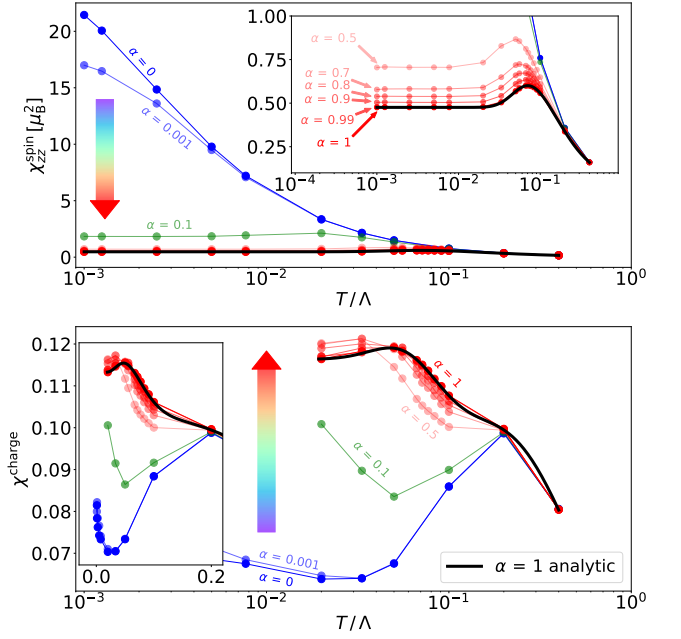


FIG. 2. Local, static spin χ_{zz}^{spin} (top) and charge χ^{charge} (bottom) susceptibility for different weights of the δ -peak with different α . We find a rapid loss of the Curie behavior with increasing α for the spin susceptibility, such that the formation of local moments is heavily suppressed. Enlarging α destroys the formation of local moments and screening effects in the charge susceptibility vanish, since only the singlet ground state remains. Model parameters: $V = 0.2\Lambda$, $U = 0.575\Lambda$ and $\Lambda = 10$ in arbitrary units of energy.

we obtain by means of the numerically exact quantum Monte Carlo (QMC) method as well as analytical and renormalization-group approaches, one more comment on TBG is in order: The singularity in $-\text{Im}\Delta(\omega)$ is present at any twist angle, but its weight and hence importance increase as one moves away from magic angle. In contrast, close to magic angle the extreme flatness of the bands lead to narrow bandwidths and small weights of the respective hybridization features. It is also important to note that the hybridization function shown in this inset of Fig. 1 ignores the back-action of the DMFT self-energy. A full analysis of this problem within DMFT is left for future work; in the present paper we are concerned with the conceptual impact on screening of a singularity at $\omega=0$ in an otherwise smooth hybridization function.

Spin and charge susceptibilities.— A convenient way of monitoring Kondo physics is calculating the spin-spin and charge-charge correlation functions on the impurity. Here, we compute the static spin- and charge-susceptibilities $\chi_{zz}^{\text{spin}}(T)$ and $\chi^{\text{charge}}(T)$ respectively, using QMC. By means of a continuous-time flavor of the QMC algorithm [29, 30] we solve at finite temperature T a single-orbital AIM with the hybridization function defined by Eq. (1) for a given α , repulsive interaction U

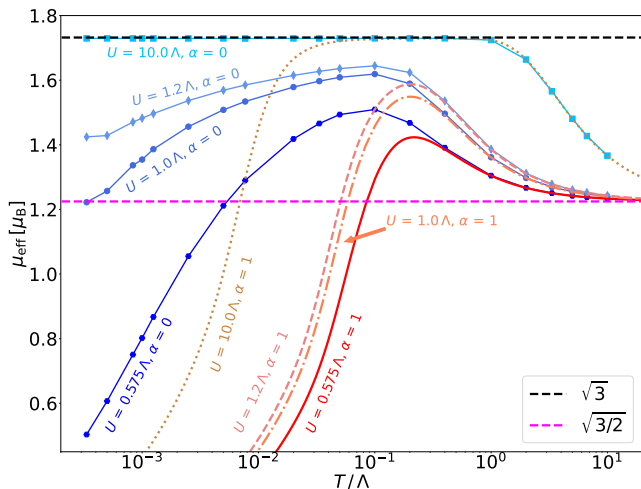


FIG. 3. Effective moment μ_{eff} of the impurity for different values of U at $\alpha = 0$ (blue) and $\alpha = 1$ (red). The large- T value corresponds to the “free-orbital” case with $\sqrt{3/2}\mu_B$; for $T \lesssim U$ we see μ_{eff} to increase upon cooling towards the Curie-Weiss value $\sqrt{3}\mu_B$ (which is only fully reached for $U = 10$). For smaller U and $\alpha=0$, the Curie-Weiss plateau is less pronounced and the drop at lower T indicates the Kondo screening. For $\alpha=1$, the loss of local moment occurs at a much higher T and almost independently on the value of U , different from the conventional $\alpha=0$ case.

and fixing the chemical potential μ to get half filling.

At intermediate-to-high temperatures, a $1/T$ Curie behavior for the spin is expected, characteristic of unscreened local magnetic moments. Upon lowering T , a crossover to a constant Pauli-like $\chi_{zz}^{\text{spin}}(T)$ signals the onset of screening of the local impurity [31–33]. Charge fluctuations are suppressed when the local moment is formed and display a minimum around T_K . Upon further lowering the temperature, a “revival” in χ^{charge} appears, as the pendant of the Pauli plateau in the spin susceptibility [34–37]. In Fig. 2, one sees this behavior for the two quantities in the case of the conventional box-like hybridization ($\alpha=0$). The deviation from the Curie law for the spin is gradual (because the temperature range of the Pauli plateau for this value of U/Λ cannot be fully reached without a time-wise highly demanding QMC calculation [30]). The minimum in the charge susceptibility is instead nicely resolved.

Surprisingly, a value for α of just 5-10% of its maximum induces a huge effect on the spin and charge responses with respect to $\alpha=0$: $\chi_{zz}^{\text{spin}}(T)$ displays an extended plateau which is reached at temperatures more than two orders of magnitude higher than the onset of Pauli behavior for $\alpha=0$. At the same time, charge fluctuations are much less suppressed and display no minimum with the “revival” upturn, as for $\alpha=0$. A δ -like peak in $-\text{Im}\Delta(\omega)$ causes therefore an unexpectedly rapid and strong qualitative deviation from the Curie behavior. This intrinsic fragility of the local moment must hence be

taken into account every time a dip in $-\text{Im}G_0(\omega)/\pi$ approaches the Fermi level.

Effective moment.— The impact of the peak in $-\text{Im}\Delta(\omega)$ on the local-moment formation can be appreciated by looking at the respective temperature dependence at different values of U . Fig. 3 shows this for $\alpha=0$ and 1. In terms of the local magnetic moment of the impurity $\mu_{\text{eff}} = g\mu_B \sqrt{S(S+1)}$, where S denotes the effective spin on the interacting site, the spin susceptibility reads $T\chi_{zz}^{\text{spin}}(T) = \mu_{\text{eff}}^2/3$. If we start from the “infinite”- T region of the interaction-scale U , all curves reach the “free” moment $\mu_{\text{eff}} = \sqrt{3/2}\mu_B$, as illustrated in Fig. 3. This corresponds to the many-body configurations with different number of electrons being only differentiated by the thermal distribution. Reducing T brings μ_{eff} up to the nominal large- U Curie-Weiss value, which for a half-filled $S=1/2$ impurity is $\sqrt{3}\mu_B$, as we are considering only the z -contribution. If the U/Λ is not huge, this value is not fully reached because of the still active charge fluctuations in the AIM. Eventually, upon further decreasing T , the screening of the moment takes place. As shown in Fig. 3, this process happens very differently between $\alpha=0$ and 1: in the conventional $\alpha=0$ case, the plateau is left only when T starts to approach the Kondo temperature from above, i.e. at temperatures that for this values of U and Λ are below $10^{-3}\Lambda$, consistent with the universal Kondo temperature curve [32, 38]. On the contrary, for $\alpha=1$, i.e. in the extreme case of a bath made of the δ function only, the loss of local moment happens at temperatures two orders of magnitude higher, with a much weaker dependence on U and with a much higher slope w.r.t. T .

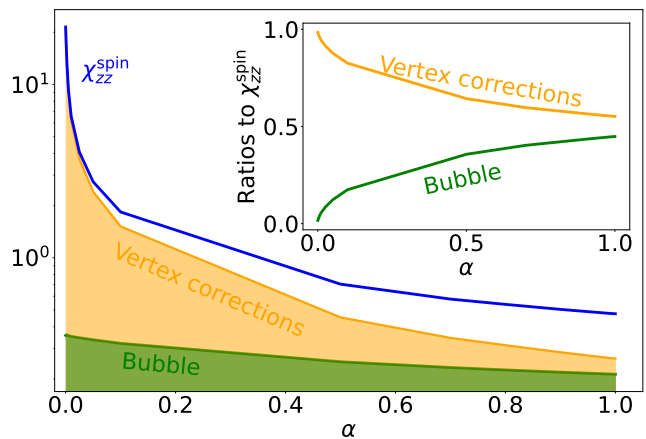


FIG. 4. Local spin susceptibility χ_{zz}^{spin} (blue) together with the corresponding contributions of bubble (green) and vertex corrections (orange) at $T = 0.001\Lambda$. The logarithmic scale evidences how the dependence on α mainly originates from the vertex corrections, which decrease very rapidly, in contrast to the rather smooth bubble term behavior. Inset: The corresponding ratios to χ_{zz}^{spin} show how the two contribution have a qualitatively different dependence on α .

Vertex corrections and bubble contribution— Physically, the loss of local moment for finite values of α can be understood as follows: A δ -like hybridization corresponds to a single isolated level. If this sits at the Fermi level as in the case of TBG at integer fillings, this level hosts one electron which has a strong tendency to form a singlet with the impurity spin [38]. Increasing the relative weight of the hybridization peak therefore reduces the many-body nature of the whole system – and hence the fluctuating local moment – very efficiently. This can be illustrated by quantifying the impact of α on the bubble of two dressed impurity Green’s function as well as on the vertex corrections, i.e. diagrams that, contrary to the bubble, have also interaction lines connecting the two dressed Green’s functions. In Fig. 4 one sees clearly how the latter, which are almost the only diagrams responsible for the local moment at $\alpha=0$ (here taking the example of $T=0.001\Lambda$) drop already by one order of magnitude at $\alpha=0.1$. At the same time the bubble contribution decreases with α very gradually instead, so that its relative importance effectively increases.

RG results.— To substantiate the above argument on the isolated bath level, we apply the renormalization group (RG). This allows us to quantify the relative importance of the hybridization to the δ -function with respect to the conventional box-like bath in driving the system towards the Kondo fixed point. For finding the flow equations we use a Kondo Hamiltonian which includes two coupling constants:

$$\hat{H} = \sum_{k,\sigma} \epsilon_k \hat{c}_{k\sigma}^\dagger \hat{c}_{k\sigma} + (1-\alpha) M \sum_{\sigma,\sigma'} \vec{S} \hat{c}_{0,\sigma}^\dagger \frac{\vec{\tau}_{\sigma,\sigma'}}{2} \hat{c}_{0,\sigma'} + \alpha M \sum_{\sigma'',\sigma'''} \vec{S} \hat{d}_{\sigma''}^\dagger \frac{\vec{\tau}_{\sigma'',\sigma'''}}{2} \hat{d}_{\sigma'''} \quad (3)$$

in standard notation, with \vec{S} the impurity spin and $\vec{\tau}$ the vector of Pauli matrices. The first coupling $J = (1-\alpha)M$ is associated to the constant hybridization, while the coupling $K = \alpha M$ is to a single fermionic level and refers to the δ -peak. $\hat{c}^{(\dagger)}$ and $\hat{d}^{(\dagger)}$ are the respective annihilation (creation) operators. Using this model, the flow equations for the dimensionless couplings $j = J/\Lambda_0$ and $k = K/\Lambda_0$ yield:

$$\begin{aligned} \beta(j) &= \Lambda \frac{dj}{d\Lambda} = -j^2, \\ \beta(k) &= \Lambda \frac{dk}{d\Lambda} = -k. \end{aligned} \quad (4)$$

These equations can be integrated to yield the running couplings:

$$j(\Lambda) = \frac{1}{\ln\left(\frac{\Lambda}{\Lambda_0}\right) + \frac{1}{j_0}}, \quad k(\Lambda) = \frac{k_0 \Lambda_0}{\Lambda}. \quad (5)$$

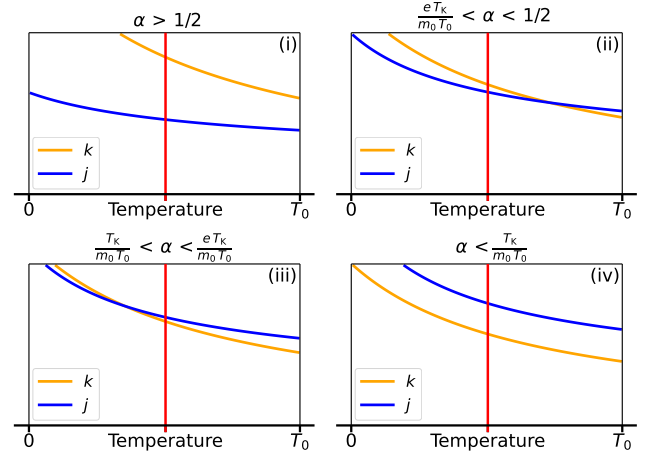


FIG. 5. Sketch of the RG flow of the dimensionless couplings k and j to the δ -peak and broad band, respectively, showing the four regimes of the δ -weight α . (i) For large α the δ -peak coupling k dominates at any T . (ii,iii) At smaller α the couplings cross as function of T , implying a crossover which is located above or below the Kondo temperature T_K (red line). (iv) For very small α the j coupling dominates at any T . We note that T_K is the Kondo temperature with respect to the j coupling, and we have extrapolated j beyond the validity of the weak-coupling result (5).

Here, we assume the initial couplings $j_0 = (1-\alpha)m_0$ and $k_0 = \alpha m_0$ with $m_0 = M_0/\Lambda_0$. By identifying the running cutoff Λ with temperature T , we use these results to deduce when conventional Kondo screening by the broad conduction band dominates over simple singlet formation with the local level described by the δ -peak or vice versa, i.e., $j > k$ or $j < k$, respectively. Four different regimes for α can be distinguished, as shown in Fig. 5: (i) At $\alpha \geq 1/2$ the δ -peak hybridization dominates the physics for all T . (ii,iii) For $T_K/(m_0 T_0) < \alpha < 1/2$ a crossover happens, with conventional Kondo effect dominating at elevated T and δ -peak hybridization winning at low T . For (ii) $\alpha > eT_K/(m_0 T_0)$ ((iii) $\alpha < eT_K/(m_0 T_0)$) this crossover happens above (below) T_K , respectively. (iv) Only for $\alpha < T_K/(m_0 T_0)$ conventional Kondo screening dominates at all T . Here, $T_K = T_0 e^{-\frac{1}{j_0}}$ denotes the Kondo temperature of the model for the j coupling, i.e., in the presence of the broad conduction band only, where the width is reduced by α .

The four different regimes can be also directly related to the behavior of the spin and charge susceptibilities in our numerical results in Fig. 2. Cases (i) and (iv) are connected to situations with $\alpha \lesssim 0.01$ and $\alpha > 1/2$, yielding the standard Kondo effect or the immediate screening of a local moment for all T , respectively. The change from regime (ii) to (iii) occurs around $\alpha \sim 0.1$.

Conclusion.— Using a combination of numerics and weak-coupling RG, we have analyzed how a δ -peak at the Fermi level in the hybridization function qualitatively alters the Kondo physics. The surprising result

of our analysis is that the local moment, as well as its gradual loss upon cooling via Kondo screening, is completely suppressed by the singular hybridization even if the relative weight of the latter is as small as about 10% of the total hybridization strength. In fact, the effects of the δ -peak become unimportant only if its weight is smaller than the dimensionless Kondo temperature associated with the non-singular part of the bath. Our results indicate a deep impact of the hybridization to such isolated bath level on the many-body nature of the Kondo effect: vertex corrections which are crucial in the conventional case to build up the local moment, are particularly fragile against the δ -peak in the bath and, hence, Kondo screening does not take place despite the still dominant weight of the non-singular bath states.

Physically, the motivation of such δ -like feature in the hybridization function comes, on the one hand, from specific molecular adsorbed complexes [26] in which there is a combination of well-behaved and sharp features in the bath which makes the interpretation of the Kondo effect less trivial. On the other hand, TBG also displays a singularity in the hybridization function of the THF model, giving relevance to our general finding for the interpretation of TBG in terms of Kondo physics [16–20].

After having assessed this fundamental repercussions of hybridizations deviating from the textbook smooth frequency dependence around ε_F , several key points will have to be addressed next. First of all, in order to understand how strongly the physics of TBG is affected by this “fragility” of the local valley/orbital moment, the feedback of the DMFT self-energy onto the hybridization function has to be taken into account. In DMFT, the bath corresponds indeed to a self-adjusting AIM and the self-energy of the THF model [16–20] and also in other models treated with DMFT [39] can either enhance or go against the peak in $-\text{Im}\Delta(\omega)$. In the study on TBG, how the fragility found here at particle-hole symmetry is modified upon departing from charge neutrality will play also a crucial role, similarly to strain, electron-phonon and long-range ordering.

We thank Sergio Caprara for useful discussions and Dumitru Călugăru for his input on the THF model for TBG. L.C. and G.S. are grateful for important conversations and collaborations with B. Andrei Bernevig, Haoyu Hu, Roser Valentí, Gautam Rai, Tim Wehling, Luca de’ Medici and Antoine Georges. We acknowledge financial support by the Deutsche Forschungsgemeinschaft (DFG, German Research Foundation) through SFB 1170 Tocotronics (project-id 258499086; MF and GS), SFB 1143 (project-id 247310070; MV), FOR 5249 (project-id 449872909, Project P05; GS), and the Würzburg-Dresden Cluster of Excellence on Complexity and Topology in Quantum Matter-ct.qmat (EXC 2147, project-id 390858490; GS and MV). SC acknowledges funding from NextGenerationEU National Innovation Ecosystem grant

ECS000000041 - VITALITY - CUP E13C22001060006 and grant PE000000023 - IEXSMA - CUP E63C22002180006. A.T. acknowledges the Austrian Science Fund (FWF) for the project I 5487 (doi: 10.55776/I5487) and I 5868 (doi: 10.55776/I5868, P1 project part of the FOR 5249 [QUAST] of the German Science Foundation, DFG). We gratefully acknowledge the Gauss Center for Supercomputing e.V. (www.gauss-center.eu) for funding this project by providing computing time on the GCS Supercomputer SuperMUC at Leibniz Supercomputing Center (www.lrz.de).

-
- [1] J. Kondo, *Progress of Theoretical Physics* **32**, 37 (1964).
 - [2] P. Coleman, *Introduction to Many-Body Physics* (Cambridge University Press, 2015).
 - [3] L. Kouwenhoven and L. Glazman, *Revival of the kondo effect* (2001).
 - [4] M. Pustilnik and L. Glazman, *Journal of Physics: Condensed Matter* **16**, R513 (2004).
 - [5] M. Pustilnik, *physica status solidi (a)* **203**, 1137 (2006).
 - [6] O. Újsághy and A. Zawadowski, *Journal of the Physical Society of Japan* **74**, 80 (2005).
 - [7] P. W. Anderson, *Phys. Rev.* **124**, 41 (1961).
 - [8] M. Jarrell, *Phys. Rev. Lett.* **69**, 168 (1992).
 - [9] M. J. Rozenberg, X. Y. Zhang, and G. Kotliar, *Phys. Rev. Lett.* **69**, 1236 (1992).
 - [10] A. Georges and W. Krauth, *Phys. Rev. Lett.* **69**, 1240 (1992).
 - [11] A. N. Rubtsov, V. V. Savkin, and A. I. Lichtenstein, *Phys. Rev. B* **72**, 035122 (2005).
 - [12] P. Werner, A. Comanac, L. de’ Medici, M. Troyer, and A. J. Millis, *Phys. Rev. Lett.* **97**, 076405 (2006).
 - [13] The Hamiltonian to calculate the hybridization function and the non-interacting spectral function for the THF model of TBG away from magic angle was taken from [18].
 - [14] D. Withoff and E. Fradkin, *Phys. Rev. Lett.* **64**, 1835 (1990).
 - [15] L. Fritz and M. Vojta, *Phys. Rev. B* **70**, 214427 (2004).
 - [16] Z.-D. Song and B. A. Bernevig, *Phys. Rev. Lett.* **129**, 047601 (2022).
 - [17] H. Hu, G. Rai, L. Crippa, J. Herzog-Arbeitman, D. Călugăru, T. Wehling, G. Sangiovanni, R. Valentí, A. M. Tsvelik, and B. A. Bernevig, *Phys. Rev. Lett.* **131**, 166501 (2023).
 - [18] D. Călugăru, M. Borovkov, L. L. H. Lau, P. Coleman, Z.-D. Song, and B. A. Bernevig, *Low Temperature Physics* **49**, 640–654 (2023).
 - [19] G. Rai, L. Crippa, D. Călugăru, H. Hu, F. Paoletti, L. de’ Medici, A. Georges, B. A. Bernevig, R. Valentí, G. Sangiovanni, and T. Wehling, *Phys. Rev. X* **14**, 031045 (2024).
 - [20] G.-D. Zhou, Y.-J. Wang, N. Tong, and Z.-D. Song, *Phys. Rev. B* **109**, 045419 (2024).
 - [21] A. Georges, G. Kotliar, W. Krauth, and M. J. Rozenberg, *Rev. Mod. Phys.* **68**, 13 (1996).
 - [22] If the AIM is obtained upon mapping a periodic lattice model onto a single site using DMFT, the lattice dispersion directly influences the functional form of $\Delta(\omega)$

- and, in particular, its frequency dependence close to $\omega=0$. In the case of linearly dispersing Dirac fermions, the hybridization function of the corresponding AIM displays a δ -function singularity at $\omega=0$ in $d=3$ and a $1/\omega$ -divergence with logarithmic corrections in $d=2$ [40]. Here we use systems such as TBG as a motivation but, for simplicity, we model $\text{Im}\Delta(\omega)$ as a box plus δ -function.
- [23] T. Pruschke, R. Bulla, and M. Jarrell, *Phys. Rev. B* **61**, 12799 (2000).
 - [24] N. Wagner, S. Ciuchi, A. Toschi, B. Trauzettel, and G. Sangiovanni, *Phys. Rev. Lett.* **126**, 206601 (2021).
 - [25] A. Mu, Z. Sun, and A. J. Millis, *Phys. Rev. B* **109**, 115154 (2024).
 - [26] J. Kügel, M. Karolak, J. Senkpiel, P.-J. Hsu, G. Sangiovanni, and M. Bode, *Nano Letters* **14**, 3895 (2014).
 - [27] M. Vojta and R. Bulla, *Eur. Phys. J. B* **28**, 283 (2002).
 - [28] A. K. Mitchell, M. Vojta, R. Bulla, and L. Fritz, *Phys. Rev. B* **88**, 195119 (2013).
 - [29] E. Gull, A. J. Millis, A. I. Lichtenstein, A. N. Rubtsov, M. Troyer, and P. Werner, *Rev. Mod. Phys.* **83**, 349 (2011).
 - [30] M. Wallerberger, A. Hausoel, P. Gunacker, A. Kowalski, N. Parragh, F. Goth, K. Held, and G. Sangiovanni, *Computer Physics Communications* **235**, 388–399 (2019).
 - [31] K. G. Wilson, *Rev. Mod. Phys.* **47**, 773 (1975).
 - [32] H. R. Krishna-murthy, J. W. Wilkins, and K. G. Wilson, *Phys. Rev. B* **21**, 1003 (1980).
 - [33] R. Bulla, T. Pruschke, and A. C. Hewson, *Journal of Physics: Condensed Matter* **9**, 10463 (1997).
 - [34] P. Chalupa, T. Schäfer, M. Reitner, D. Springer, S. Andergassen, and A. Toschi, *Phys. Rev. Lett.* **126**, 056403 (2021).
 - [35] T. B. Mazitov and A. A. Katanin, *Phys. Rev. B* **105**, L081111 (2022).
 - [36] C. Melnick and G. Kotliar, *Phys. Rev. B* **101**, 165105 (2020).
 - [37] S. Adler, F. Krien, P. Chalupa-Gantner, G. Sangiovanni, and A. Toschi, *SciPost Physics* **16**, 10.21468/scipost-phys.16.2.054 (2024).
 - [38] A. C. Hewson, *The Kondo Problem to Heavy Fermions*, Cambridge Studies in Magnetism (Cambridge University Press, 1993).
 - [39] A. Datta, M. J. Calderón, A. Camjayi, and E. Bascones, *Nat. Commun.* **14**, 5036 (2023).
 - [40] M. Vojta, A. K. Mitchell, and F. Zschocke, *Phys. Rev. Lett.* **117**, 037202 (2016).